NEW TRENDS IN HIGH-ENERGY PHYSICS

Budva, Becici, Montenegro
24–30 September 2018

Proceedings of the Conference

JOINT INSTITUTE FOR NUCLEAR RESEARCH

NEW TRENDS IN HIGH-ENERGY PHYSICS

Budva, Becici, Montenegro
24–30 September 2018

Proceedings of the Conference

Dubna 2019

УДК 539.1(063)
ББК 22.3я431
N52

The contributions are reproduced directly from the originals.

New Trends in High-Energy Physics: Proceedings of the Conference
N52 (Budva, Becici, Montenegro, 24–30 September 2018). — Dubna: JINR, 2019. — 287 p.

ISBN 978-5-9530-0509-8

The Conference on New Trends in High-Energy Physics organized by the Joint Institute for Nuclear Research, Dubna, and Bogolyubov Institute for Theoretical Physics, National Academy of Sciences of Ukraine, was held at the Hotel Splendid, Conference Hall, Budva, Becici, Montenegro, on 24–30 September 2018.

The present Proceedings contain direct reproductions of authors' originals (reviews and short communications) that arrived at the Organizing Committee and are grouped somewhat loosely. We have united a number of sections. The contributions within each section are ordered according to the conference program. The Organizing Committee thanks all participants for their contributions. More conference information and pictures can be found on our site: http://indico-new.jinr.ru/event/ntihep2018.

Новые тенденции в физике высоких энергий: Труды конференции (Будва, Бечичи, Черногория, 24–30 сентября 2018 г.). — Дубна: ОИЯИ, 2019. — 287 с.

ISBN 978-5-9530-0509-8

Конференция «Новые тенденции в физике высоких энергий», организованная Объединенным институтом ядерных исследований (Дубна) и Институтом теоретической физики им. Н. Н. Боголюбова НАН Украины (Киев), проходила в конференц-зале гостиницы «Splendid» (Будва, Бечичи, Черногория) 24–30 сентября 2018 г.

Данный сборник содержит материалы (обзоры и короткие сообщения), присланные авторами в оргкомитет, сгруппированные в свободном порядке, ряд разделов объединен. Статьи в каждом разделе упорядочены в соответствии с программой конференции. Оргкомитет благодарит за сотрудничество всех участников. Более подробную информацию о конференции, а также фотографии можно найти на сайте: http://indico-new. jinr.ru/event/ntihep2018.

УДК 539.1(063)
ББК 22.3я431

ISBN 978-5-9530-0509-8

CONTENTS

III. "NEW COLLIDERS, FACILITIES, DETECTORS, COMPUTING AND DATA ANALYSES TECHNIQUES"

Diffraction in lepton-hadron and hadron-hadron scattering

Roberto Fiore
Department of Physics, University of Calabria, I-87036 Arcavacata di Rende, Cosenza, ITALY
robertofiore1943@gmail.com

László Jenkovszky
Bogolyubov Institute for Theoretical Physics (BITP),
14-b, Metrologicheskaya str., Kiev, 03680, UKRAINE
jenk@bitp.kiev.ua

Nadya Maslova
Physics Department, Taras Shevchenko National University of Kyiv,
03127, Kyiv, Hlushkova Avenue, 4, UKRAINE
nadiiamaslova@gmail.com

Rainer Schicker
Physikalisches Institut, Im Neuenheimer Feld 226,
Heidelberg University, 69120 Heidelberg, GERMANY
schicker@physi.uni-heidelberg.de

Jolán Turóci
Uzhhorod National University,
14, Universytetska str., Uzhgorod, 88000, UKRAINE
turocijolika@gmail.com

We study diffractive phenomena in proton-proton and electron-proton collisions at the LHC and DESY using analyticity, crossing symmetry and unitarity, particularly the Regge-pole model realizing these concepts. Fits to the data are presented and tensions between theoretical predictions and the data that may indicate the way to further progress are in the focus of our paper. Elastic *pp* (LHC) and DIS *ep* scattering (DESY) usually are considered by means of two pomerons, "soft" and "hard" or with a single one, but varying intercept. We introduce a reggeometric pomeron replacing the above objects.

Keywords: LHC; Regge-poles; pomeron; odderon; duality; unitarity; diffraction; CED; DIS.

1. Introduction

In this paper we present our study of diffractive proton-proton and electron-proton collisions in the framework of the Regge pole model (we recall that Regge poles lie on the so called Regge trajectories $\alpha(t)$, in the t channel) through the introduction of a reggeometric pomeron $\alpha_P(t)$. First of all, we start with a brief recapitulation of the present state of the theory. The construction of the scattering amplitude implies two steps: choice of the input (Born term) and subsequent unitarization. The better the input (*i.e.*,the closer to the expected unitary output), the better are the chances of a successfully converging solution (*i.e.*, the smaller are the unitarity corrections). The standard procedure is to use a simple Regge-pole amplitude as input with subsequent eikonalization.

The common feature in many papers studying this problem (see Refs. 1-7) is the use of a supercritical pomeron, $\alpha_P(t=0) > 1$, as input, motivated by the rise of the cross sections

and by perturbative QCD calculations (for instance, Ref. 8, where the BFKL theory is introduced). The next indispensable step is unitarization, usually realized in the eikonal formalism. Unitarization is necessary at least for two reasons: to reconcile the rise of the total cross sections with the Froissart-Martin bound and to generate the diffractive dip-bump structures in the differential cross sections. The latter issue is critical for most of the theoretical constructions since the standard eikonalization procedure results in a sequence of secondary dips and bumps, while experimentally a single dip-bump is observed only, as confirmed by all measurements including those recent, at highest LHC energy. This deficiency is usually resolved e.g. by introducing the so-called enhanced diagrams, or extra free parameters. Still, none of the above-mentioned models was able to reproduce the whole set of pp and $p\bar{p}$ a data from the ISR to the LHC in the dip-bump region. This is a crucial test for all existing models. These models did not predict the unexpected rapid rise, as $\ln^2 s$, of the forward slope revealed by the experiment TOTEM (see Ref. 9) or the drastic decrease of the parameter $\rho(s, 0)$, ratio of the real to imaginary part of the elastic scattering amplitude, reported in Ref. 10. The latter (a single data point) was fitted a posteriori by an odderon [11], although in an earlier paper by one of the authors the model predicted quite a different trend. To summarize, the existing Regge-eikonal models are compatible with the general trend of high-energy diffractive scattering, but many details, such as the dynamics of the dip-bump, the role of the odderon still remains open and controversial.

The TOTEM Collaboration announced [12] new results of the measurements on the proton-proton elastic slope at 7 and 8 TeV, B(7 TeV)= 19,89$\pm$0,27 and B(8 TeV)= 19,9$\pm$0,3 GeV^{-2}, showing that the logarithmic approximation, with a ln(s) behavior, an exponential fit over the large |t|-range from 0.005 to 0.2 GeV^2 describes the differential distribution well. These data offer new information concerning the burning problem of the strong interaction dynamics, namely the onset of (or the appoach to) the asymptotic regime of the strong interaction.

The approach to the expected asymptotic behavior has two stages. One is the onset of pomeron dominance, *i.e.*, of the domain where secondary reggeon contributions become negligible. It can be shown that in the nearly forward direction, at LHC energies the contribution from secondary trajectories is negligible, smaller than the error bars in the measured total cross section, *i.e.* "soft" physics at the LHC is pomeron-dominated. The next question is where does the pomeron itself reaches its asymptotics. Below we address these questions.

2. *S*-matrix theory, Regge-pole models

Regge-pole theory is the adequate tool to handle "soft" or "forward" physics. It is a successful example of the analytic S-matrix theory, based on analyticity, unitarity and crossing symmetry of the scattering amplitude. It was developed in the 60-ies of the past century, culminating in discovery of duality and dual amplitudes, whereupon, in the 70-ies was overshadowed by local quantum eld theories, more specifically by quantum chromodynamics (QCD).

2.1. Regge poles and trajectories; factorization

Below we introduce the Regge-pole model with emphases on its practical applications. Its derivation from potential scattering, the Schrödinger equation and its relation to quantum mechanics can be found in many textbooks (see, e.g., Refs. 13-15).

In relativistic S-matrix theory we do not have a Schrödinger equation, and the existence of Regge poles is conjectured by analogy with quantum mechanics. The use of the complex angular moments results (for details, see Refs.13-15) in a representation for the amplitude,

$$A(s,t) = \beta(t)\xi(t)s^{\alpha(t)},$$

valid in all channels, where $\beta(t)$ is the residue and

$$\xi(t) = -\frac{1 \pm e^{-i\pi\alpha(t)}}{sin\pi\alpha(t)}$$

is the signature factor.

Baryon and meson trajectories are nearly linear functions in a limited range of their variables. This is suggested by the (nearly) exponential shape of forward cone in elastic scattering and by the meson and baryon spectrum. In Fig. 1 a typical Chew-Frautschi plot is shown. Similar nearly linear plots are known for other mesons and baryons [13-15]. Whatever appealing, this simplicity is only an approximation to reality: analyticity and unitarity as well as the finiteness of resonances require Regge trajectories to be non-linear complex functions (see, for instance, Refs. 16-18**)**.

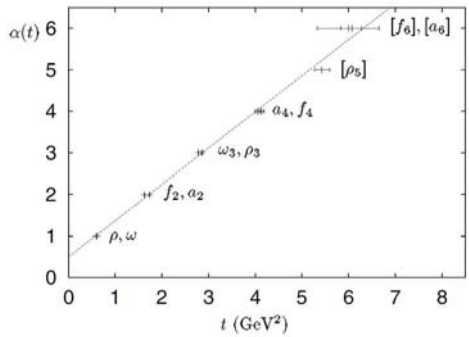

Fig. 1. Linear mesonic Chew-Frautschi plot (spin vs. squared masses, $Re\alpha(t)$).

Let us reiterate that Regge trajectories are building blocks of the scattering amplitude. In dual models (see below) they appear as the only variables. By crossing symmetry, they connect (smoothly interpolate between) the resonance formation – which implies positive *x*=*s* or *t*) with scattering (negative *x*), thus anticipating duality.

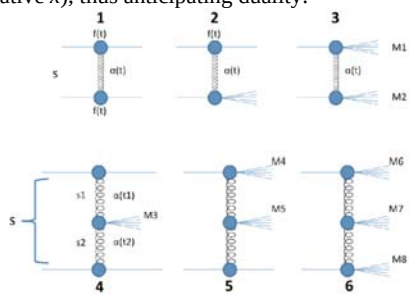

Fig. 2. Diagrams describing Regge-pole factorization.

Factorization of the Regge residue $\beta(t)$ and the "propagator" $(s/s_0)^{\alpha_P(t)-1}$ is a basic property of the theory (see Ref. 14). As mentioned, at the LHC for the first time, we have the opportunity to test directly Regge-factorization in diffraction, since the scattering amplitude here is dominated by a pomeron exchange, identical in elastic and inelastic diffraction. Simple factorization relations between elastic $d\sigma_{el}/dt$, single σ_{SD}/dt and double $d^3\sigma_{DD}/dtM_1^2dM_2^2$

cross-sections are known from the literature [19]. By writing the scattering amplitude as a product of vertices, the elastic f and the inelastic F, multiplied by the (universal) propagator (pomeron exchange), $f^2 s^\alpha$, fFs^α, $F^2 s^\alpha$, respectively for the elastic scattering, single (SD) and double (DD) diffraction dissociation (see Fig. 2) one gets

$$\frac{d^3\sigma_{DD}}{dtdM_1^2 dM_2^2} = \frac{\frac{d^2\sigma_{SD_1}}{dtdM_1^2}\frac{d^2\sigma_{SD_2}}{dtdM_2^2}}{\frac{d\sigma_{el}}{dt}}. \quad (1)$$

Assuming exponential residua $\exp(Bt)$ for both the elastic scattering and SD, and integrating over t one obtains

$$\frac{d^3\sigma_{DD}}{dM_1^2 dM_2^2} = \frac{k\frac{d^2\sigma_{SD_1}}{dM_1^2}\frac{d^2\sigma_{SD_2}}{dM_2^2}}{\frac{d\sigma_{el}}{dt}}, \quad (2)$$

where

$$k = r^2/(2r-1), r = B_{SD}/B_{el}.$$

To summarize this discussion, we emphasize the important role of the ratio between the inelastic and elastic slope, which at the LHC is close to its critical value, $B_{SD}/B_{el} = 0.5$, which means a very sensitive correlation between these two quantities. The right balance may require a correlated study of the two quantities, by keeping the ratio above 0.5. This constrain may guide future experiments on elastic and inelastic diffraction.

2.2. Pomeron and odderon

Regge trajectories (reggeons), introduced in the 60-ies of the past century correspond to a family of mesons or baryons sitting on the real part of the trajectories – the so-called Chew-Frautschi plot, to which their parameters (intercept and slope) are adjusted. There are two exceptions, namely the pomeron and odderon. The pomeron was introduced by I.Ya. Pomeranchuk as a fictive trajectory with postulated unit intercept to provide for non-decreasing asymptotic total cross-sections. In those days, the common belief was that asymptotically the cross sections tend to a constant limit. This has changed after the rise of cross sections was discovered at the ISR. The new, fictitious trajectory accommodates the asymptotically constant or rising cross section provided its intercept is respectively one or bigger, $\alpha_P(0) \geq 1$. The so-called supercritical pomeron, typically with $\alpha_P(0) \approx 1.1$ violates the Froissart bound (and unitarity) at very high energies, beyond any credible extrapolation. Nevertheless, formally and for aesthetic reasons, the input amplitude should be subjected to unitarization.

Unlike the case of ordinary (called also secondary or sub-leading) reggeons the pomeron trajectory was considered, since the beginning, as not connected to any observed particle. This assumption changed in the 70-ies with the advent of the quark model and the QCD. Nowadays the pomeron trajectory has its own Chew-Frautschi plot with glueballs, bound states of gluons. Glueballs are eventually mixed with quarks, forming "hybrids": this makes difficult their experimental identification.

The existence of the pomeron makes plausible the existence of its odd-C counterpart – the odderon. While the pomeron is made of an even number of gluons, the odderon is a bound state of an odd number of gluons. Moreover, the pomeron is "seen" as the imaginary part of the forward amplitude (total cross section), instead the identification of the odderon is not so unique.

2.3. Duality

The notion of duality, discovered in 1968 [20], has many facets values. Here we deal with resonance-Regge duality (or the Veneziano model [21]), discovered by saturating the so-called nite energy sum rules. Their analysis showed that, contrary to expectations, the proper sum of resonances produces a smooth Regge behavior and vice versa, their sum producing double counting. As a next step, an explicit dual amplitude was constructed. It is an Euler *B*-function:

$$A(s,t) = \int_0^1 dx x^{-\alpha(s)-1}(1-x)^{\alpha(t)-1} = B(-\alpha(s),-\alpha(t)) = \frac{\Gamma(-\alpha(s))\Gamma(-\alpha(t))}{\Gamma(-\alpha(s)-\alpha(t))}. \quad (3)$$

The Veneziano amplitude has several remarkable properties: it is crossing symmetric by construction, can be expanded in a pole series (resonance poles) in the *s* and *t* channel, and at large *s*, by the Stirling formula it is Regge-behaved, thus explicitly showing resonance-Regge duality - see, for instance, Fig. 3. At the same time, the model is not free from difficulties or limitations: it is valid only in the so-called narrow-resonance approximation, bringing to real and linear trajectories only, and as a result analyticity and unitarity are violated. A solution was found in dual amplitudes with Mandelstam analyticity (DAMA) [22], replacing Eq. (3) with

$$A(s,t) = \int_0^1 dx \left(\frac{x}{g}\right)^{-\alpha(s,x)-1} \left(\frac{1-x}{g}\right)^{\alpha(t,1-x)-1}, \quad (4)$$

where g > 1 is a parameter.

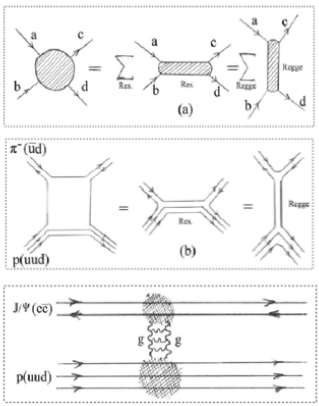

Fig. 3. Diagrams describing the resonance-Regge duality

Its low-energy pole decomposition the amplitude has the form

$$A(s,t) = \sum_{n=0}^{\infty} g^{n+1} \sum_{l=0}^{n} [-s\alpha(s)]^l \frac{C_{n-l}(t)}{[n-\alpha(s)]^{l+1}}, \quad (5)$$

where $C_{n-l}(t)$ is the residue, whose form is fixed by the *t*-channel Regge trajectory.

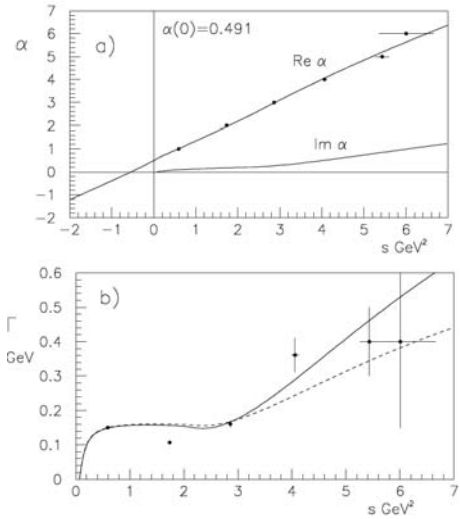

Fig. 4. (a) Re $\alpha(s)$ and Im $\alpha(s)$ for the degenerate $\rho - a_2$ trajectory; (b) continuous line: Γ(s) for the degenerate $\rho - a_2$ trajectory, dashed line: Γ(s) for the nondegenerate ρ trajectory.

As an example of typical terms in Eq. 3, in Fig. 4 we present the Chew-Frautschi plot of the degenerate $\rho - a_2$trajectory (real and imaginary parts) in Fig. 1(a), together with, in Fig. 1(b) the width $\Gamma(s)$ for the degenerate $\rho - a_2$ trajectory (continuous line) and the nondegenerate ρ trajectory (see, on this, Ref. 23), by means of a dispersion relation.

Resonance-Regge duality is applicable also in relating resonances in the missing mass of the DD to the high-mass smooth asymptotics, as shown in Fig. 5.

Finally, we mention the parton-hadron (Bloom-Gilman) duality [24]: it relates resonance production in deep-inelastic scattering to the smooth scaling behaviour of structure functions and may be a clue to the confinement problem!

2.4. Geometry and the black disc limit

The unitarity condition is simple in the impact parameters representation of the scattering amplitude; it is

$$h(s,b) = \frac{1}{4s}\int \frac{d^2\vec{k}}{(2\pi)^2} e^{i\vec{k}\vec{b}} A(s,t) = \frac{1}{8\pi s}\int_0^\infty dk k J_0\left(b\sqrt{-t}\right) A(s,t)\,, \tag{6}$$

with the inverse transformation

$$A(s,t) = 16\pi^2 s \int \frac{d^2\vec{b}}{(2\pi)^2} e^{-i\vec{k}\vec{b}} h(s,b) = \frac{1}{8\pi s}\int_0^\infty db b J_0\left(b\sqrt{-t}\right) h(s,b)\,. \tag{7}$$

In these equations $h(s,b)$ is called elastic impact parameter profile, *A(s,t)* is the elastic amplitude, $J_0(z)$ is the Bessel function of the zeroth order, $\vec{k}$ is a two-dimensional vector, $t \approx -k_\perp^2$ and *b* is the impact parameter.

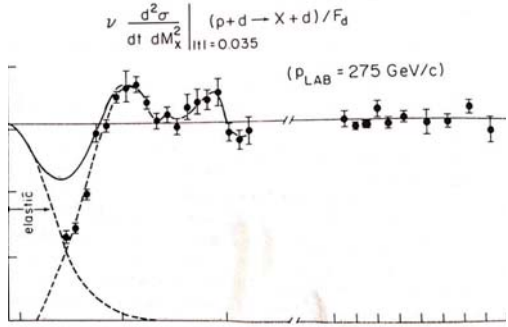

Fig. 5. Finite-mass sum rules (FMSR), Ref. 17, relating low missing-mass resonances (horizontal axis) with high mass production (vertical axis) in diffraction dissociation, are shown.

For the observables the following expressions hold, see Refs. 5-7:

$$\sigma_t(s) = \frac{1}{s} ImA(s,0) = 8\pi \int_0^\infty dbb Imh(s,b), \tag{8}$$

$$\sigma_{el}(s) = \frac{1}{16\pi s^2} \int_{-\infty}^0 dt |A(s,t)|^2 = 8\pi \int_0^\infty dbb |h(s,b)|^2, \tag{9}$$

$$\sigma_{inel}(s) = 8\pi \int_0^\infty dbb (Imh(s,b) - |h(s,b)|^2)\,, \tag{10}$$

where, in the impact parameter *b* representation, *h*(*s*, *b*) is the elastic-scattering amplitude at the center-of-mass energy and *Imh*(*s*, *b*), usually called the profile function, represents the hadron opacity. The eikonal and u matrix approaches differ dramatically concerning the "black disc limit", absolute in the eikonal model, but merely transitory for the u matrix. A large number of paper appeared, e.g. Refs. 5-7, dramatizing the "dangerous" vicinity of the black disc limit $Imh(s,b) = 0.5$, reached or even crossed at the LHC. The transformation of the experimental data, including the differential cross sections measured at the LHC can be always questioned because the real part of the amplitude (or the phase) is not measured directly.

Contrary to the eikonal, in the u matrix approach the black disc is not an absolute limit. Having reached $Imh(s,0) = 0.5$, the nucleon will tend to be more transparent [25]. This phenomenon was discussed in a number of papers by S.M. Troshin and N.E. Tyurin (see, for instance, Ref. 25 and references therein). In Sec. 3 we come back to the predictions of this unorthodox unitarization scheme.

3. Unitarity and "asymptopia"

3.1. Unitarity

We find approximate solutions of the u-matrix unitarization with a double pole (DP) as input. Postponing a detailed fit to the data, here we explore the general trend in the behavior of the observables, concentrating on the expected transition to the asymptotic regime of the strong interaction.

In the u matrix approach, the unitarized amplitude is [25]

$$h(\rho,s) = \frac{u(\rho,s)}{1 - iu(\rho,s)}\,, \tag{11}$$

where $u(\rho, s)$ is the input "Born" term.

We obtain for the forward measurables, in the $O(L^{-1})$ approximation ($L = \ln(s/s_0)$, s_0 being a scale for the square of the total energy s)

$$\sigma_{tot} = \frac{4\pi\alpha'_P}{\lambda}\ln(1+g)\,(1+\lambda L), \tag{12}$$

$$\sigma_{in} = \frac{4\pi\alpha'_P}{\lambda}\frac{g}{1+g}(1+\lambda L)\,, \tag{13}$$

$$\sigma_{el} = \frac{4\pi\alpha'_P}{\lambda}\left(\ln(1+g) - \frac{g}{1+g}\right)(1+\lambda L)\,, \tag{14}$$

where λ is a parameter, whose typical value is 0.06 [17].

One can see from Eqs. (12)-(14) that, in the leading $O(L^{-1})$ approximation, the energy dependence of the cross sections is not affected by unitarization if g is constant, that was typical for the ISR era with geometrical scaling (GS). The GS is violated beyond the ISR energies, requiring the energy dependence, $g \to g(s)$, to be discussed in what follows.

Furthermore, in the *O(1/L)* approximation, the amplitude can be written as

$$A(s,0) = A_B(s,0)\frac{\ln(1+g)}{g}\ . \tag{15}$$

In the "Born approximation" we have the McDowell-Martin limit [26] for the slope:

$$B(s,0) = \frac{\sigma_{tot}^2(1+\rho^2)}{16\pi\sigma_{el}}\ . \tag{16}$$

The parameter g may be found from the ratio

$$\frac{\sigma_{el}}{\sigma_{tot}} = 1 - \frac{g}{(1+g)\ln(1+g)}, \tag{17}$$

where g is constant in the case of unit dipole pomeron (DP) intercept, sharing the property of geometrical scaling (GS), typical of the ISR energy region, with

$$\sigma_t \sim \sigma_{el} \sim \sigma_{in} \sim B(s) \sim \ln(s). \tag{18}$$

Beyond the ISR the ratio (17) starts rising, braking the GS. This phenomenon is related with the rise of the parameter *g(s);* that can be calculated (and parametrized) uniquely from the experimental data on the the ratio (17). Consequently, the GS relation will be replaced by the asymptotic formulas to be discussed in the next Subsection.The results of the "perturbative" (due to smalleness at high energies of the parameter L^{-1}) expansion are attractive for their simplicity and the possibility to perform the calculations analytically. Evaluation of higher-order, subleading corrections is possible but was not done as yet. Even more interesting are exact numerical calculations with simultaneous fits to the date. They are feasible, although require huge machine resources (two-fold numerical Fourier-Bessel transforms with minimization (through MINUIT procedure at each step).

3.2. Asymptotic universality

In this Subsection we use the obtained results to predict future trends. Our first conclusion is the existence of two regimes: the first is the "low-energy" ISR-FNAL region, which shows modest (logarithmic) rise of the cross section with constant ratios σ_{el}/σ_{tot} and σ_{tot}/B, i.e. GS; the second is asymptotic, with Froissart saturation and $\sigma_{el}/\sigma_{tot} \to 1$. The transition between the two regimes and the onset of the asymptotic behavior is quantified by the "running constant" *g(s)*.

One can see from Eq. (12) that the rise of σ_{tot} is a combined effect coming from two factors: increasing intensity of the interaction $\mathcal{L}_1 = ln[1 + g(s)]$ and increasing interaction radius $\mathcal{L}_2 = 1 + \lambda L$. Their product results in the Froissart saturation,

$$\sigma_{tot} \sim c ln^2 s. \tag{19}$$

Eq. (19) relates the coefficient *c* with the slope of the pomeron trajectory α'_P. Setting $\alpha'_P = 0.394$ GeV^{-2}, we get $c = 0.088$ mb, close to its fitted value.

4. Diffractive deep-inelastic scattering: how many pomerons?

Let us establish two postulates:

1. Regge factorization holds, *i.e*. the dependence on the virtuality of the external particle (virtual photon) enters only the relevant vertex, not the propagator;
2. there is only one pomeron in Nature and it is the same in all reactions. It may be complicated, e.g. having many, at least two, components (soft and hard?).

The first postulate was applied, for example, in Refs. 27 and 28 to study the deeply virtual Compton scattering (DVCS) and the vector meson production (VMP). In Fig. 6, where diagrams (a) and (b) represent the DVCS and the VMP, respectively, the Q^2 dependence enters only the upper vertex of the diagram (c), where we explicitate the Regge-factorized form of the amplitude for both processes. The particular form of this dependence and its interplay with t is not unique.

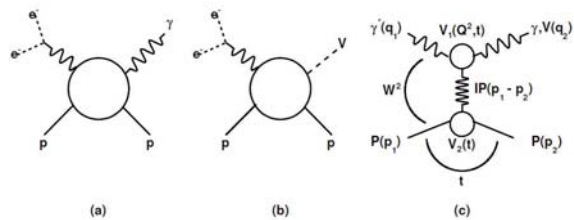

Fig. 6. Diagrams of DVCS (a) and VMP (b); (c) DVCS (VMP) amplitude in a Regge-factorized form

Hadron-hadron elastic scattering is different from exclusive VMP and DVCS not only because the photon is different from a hadron (although they are related by vector meson dominance), but even more because of the transition between space-and time-like regions: while the virtual photon's "mass square" q^2 is negative, that of the hadron is positive and that makes this attempt interesting!

4.1. Reggeometric pomeron

We start by reminding the properties and some representative results of the single-term Reggeometric model (see Ref. 27).

The invariant scattering amplitude is defined as

$$A(Q^2,s,t) = \widetilde{H} e^{-i\pi\alpha(t)/2} \left(\frac{s}{s_0}\right)^{\alpha(t)} e^{2\left(\frac{a}{Q^2}-\frac{b}{2m_N^2}\right)t}. \tag{20}$$

Here

$$\alpha(t) = \alpha_0 + \alpha' t \tag{21}$$

is the linear pomeron trajectory, a and b are two parameters to be determined with the fitting procedure and m_N is the nucleon mass. The coefficient $\widetilde{H}$ is a function providing the right behavior of elastic cross section in $\tilde{Q}^2 = Q^2 + M_V^2$ (M_V being the vector meson mass):

$$\widetilde{H} \equiv \widetilde{H}(\tilde{Q}^2) = \frac{\widetilde{A_0}}{\left(1+\frac{\tilde{Q}^2}{Q_0^2}\right)^{n_S}}, \tag{22}$$

where $\widetilde{A_0}$ is a normalization factor, Q_0^2 is a scale for the virtuality and n_S is a real positive number. Notice that we use the variable $\tilde{Q}^2$ as a measure of "hardness". By using Eq. (22) with the norm and

$$\frac{d\sigma_{el}}{dt} = \frac{\pi}{s^2}|A(Q^2,s,t)|^2, \tag{23}$$

the differential and integrated elastic cross sections become

$$\frac{d\sigma_{el}}{dt} = \frac{A_0^2}{\left(1+\frac{\tilde{Q}^2}{Q_0^2}\right)^{2n}} \left(\frac{s}{s_0}\right)^{2(\alpha(t)-1)} e^{4\left(\frac{a}{Q^2}-\frac{b}{2m_N^2}\right)t} \tag{24}$$

and

$$\sigma_{el} = \frac{A_0^2}{\left(1+\frac{\tilde{Q}^2}{Q_0^2}\right)^{2n}} \frac{\left(\frac{s}{s_0}\right)^{2(\alpha_0-1)}}{4\left(\frac{a}{Q^2}-\frac{b}{2m_N^2}\right)+2\alpha' ln\left(\frac{s}{s_0}\right)}, \tag{25}$$

where

$$A_0 = -\frac{\sqrt{\pi}}{s_0}\widetilde{A_0}.$$

Eqs. (24) and (25) (for simplicity we set $s_0 = 1\ \mathrm{GeV}^2$) were fitted [29] to the HERA data obtained the by ZEUS and H1 Collaborations on exclusive diffractive VMP.

A shortcoming of the single-term Reggeometric pomeron model, expressed by Eq. (20), is that the fitted parameters in this model acquire particular values for each reaction.

4.2. Two-component Reggeometric pomeron

In this Subsection we try to approach a complicated and controversial subject, namely the existence of two (or more) different pomerons: one "soft" responsible for on-mass-shall hadronic reactions, and the other one(s) "hard" applicable to of-mass-shall deep inelastic

scattering (DIS). There are similarities between the two soft and hard models (e.g., Regge behavior), but also differences. The main difference is that the Regge pole model, being part of the analytic S matrix theory, strictly speaking, is applicable to asymptotically free states on the mass shall only. Another difference is that the hard (or "Lipatov") pomeron is assumed to follow from the local quantum field theory (QCD) with confined quarks and gluons. We do not know how can these two extremes be reconciled. Below we try to combine these two approaches by using a specific model, a "handle" combining three independent variables: *s*, *t* and Q^2:

We introduce an universal, "soft" and "hard", pomeron model (see Ref. 27). Using the Reggeometric ansatz expressed by Eq. (20), the amplitude is written as a sum of two parts, corresponding to the "soft" and "hard" components of a universal, unique pomeron:

$$A(Q^2,s,t) \equiv A_s(Q^2,s,t) + A_h(Q^2,s,t) =$$

$$\widetilde{H_s} e^{-i\frac{\pi}{2}\alpha_s(t)} \left(\frac{s}{s_{os}}\right)^{\alpha_s(t)} e^{2\left(\frac{a_s}{Q^2}-\frac{b_s}{2m_N^2}\right)t} +$$

$$\widetilde{H_h} e^{-i\frac{\pi}{2}\alpha_h(t)} \left(\frac{s}{s_{os}}\right)^{\alpha_h(t)} e^{2\left(\frac{a_h}{Q^2}-\frac{b_h}{2m_N^2}\right)t} . \qquad (26)$$

Here s_{os} and s_{oh} are squared energy scales, and a_i and b_i, with i=*s*,*h*, are parameters to be determinated with the fitting procedure. The two coefficients $\widetilde{H_s}$ and $\widetilde{H_h}$ are functions similar to those defined in Ref. 25.

Each component of Eq. (26) has its own, "soft" or "hard", pomeron linear trajectory:

$$\alpha_s(t) = \alpha_{os} + \alpha'_s t, \qquad \alpha_h(t) = \alpha_{oh} + \alpha'_h t.$$

As input we use the parameters suggested by Donnachie and Landshoff [30], so that

$$\alpha_s(t) = 1.08 + 0.25t, \qquad \alpha_h(t) = 1.40 + 0.1t.$$

Let us illustrate the important and delicate interplay between the "soft" and "hard" components of our unique pomeron. Since the amplitude consists of two parts, according to Eq. (26), it can be written as

$$A(Q^2,s,t) = A_s(Q^2,s,t) + A_h(Q^2,s,t) . \qquad (27)$$

As a consequence, the differential and elastic cross section contain also an interference term between the "soft" and "hard" parts, so that they read

$$\frac{d\sigma_{el}}{dt} = \frac{d\sigma_{s,el}}{dt} + \frac{d\sigma_{h,el}}{dt} + \frac{d\sigma_{interf,el}}{dt} \qquad (28)$$

and

$$\sigma_{el=}\sigma_{s,el} + \sigma_{h,el} + \sigma_{interf,el} . \qquad (29)$$

Given Eqs. (28) and (29), we can define the following ratios for each component:

$$R_i\left(\widetilde{Q^2},W,t\right) = \frac{\frac{d\sigma_{i,el}}{dt}}{\frac{d\sigma_{el}}{dt}} \qquad (30)$$

and

$$R_i\left(\widetilde{Q^2}, W\right) = \frac{\sigma_{i,el}}{\sigma_{el}}, \tag{31}$$

where *i* stands for *s*, *h*, *interf.*

Fig. 7 shows the interplay between the components for both $\sigma_{i,el}$ and $R_i\left(\tilde{Q}^2, t\right)$, as function of $\tilde{Q}^2$, for $W = 90$ GeV. In Fig. 8. both diagramts show that not only $\tilde{Q}^2$ is the parameter defining softness or hardness of the process, but such is also the combination of $\tilde{Q}^2$ and *t*, similar to the variable $z = t - Q^2$ introduced in Ref. 27. On the whole, it can be seen from the diagrams that the soft component dominates in the region of low $\tilde{Q}^2$ and *t*, while the hard component dominates in the region of high $\tilde{Q}^2$ and *t*.

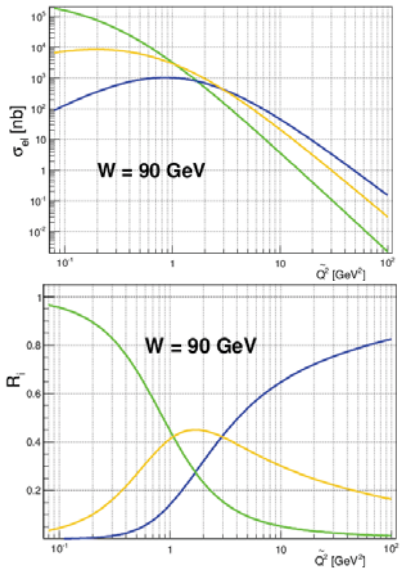

Fig. 7. Interplay between soft (green line), hard (blue line) and interference (yellow line) components of the cross section $\sigma_{i,el}$ (upper Figure) and the ratio $R_i\left(\tilde{Q}^2, t\right)$ (lower Figure) as function of $\tilde{Q}^2$, for W = 90 Gev.

5. Conclusions

The total, elastic and inelastic cross sections at the LHC did not reveal surprises; the rate of their rise (not predicted by the theory) follows extrapolations of phenomenological models, typically $\ln^2 s$ or, equivalently that of Donnachie and Landshoff 's supercritical pomeron with $\alpha(0) \approx 0.08$.

Forward physics at the LHC is dominated by the pomeron exchange, the role of secondary (e.g. f of ρ) exchanges is negligible, their relative contribution there being smaller than the experimental uncertainties. The odderon is not “seen” in fits to total cross sections. Although the common belief is that cross sections will continue rising indefinitely, alternatives, e.g. tending to a constant, oscillations etc. are not excluded by the theory.

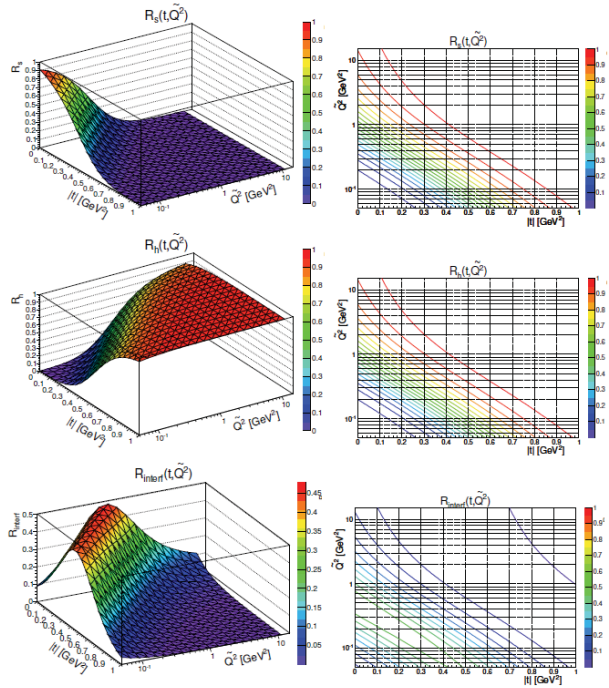

Fig. 8. Left column: soft (upper surface), hard (middle surface) and interference (bottom surface) components of the ratio $R_i(\tilde{Q}^2, W, t)$ are shown as functions of $\tilde{Q}^2$ and t, for W=90 GeV. Right column: some representative curves of the surfaces projected onto the $(t, \widetilde{Q^2})$ plane.

Contrary to total cross sections, the data on the forward slope $B(s,0)$ and the phase (the $\rho(s,0)$ parameter) offers surprises, triggering theoretical work. The forward slope $B(s,0)$, typically logarithmic in Regge-pole models, was found by the TOTEM collaboration to accelerate from $\ln(s)$ to $\ln^2(s)$ at highest LHC energy [9,12], needing theoretical explanation and understanding. Another news from TOTEM is the surprisingly low value $\rho(13,0) = 0.10\pm0.01$ [10]. The low value of the ratio $\rho(13,0)$ is almost a direct evidence for the odderon, predicted many years ago and discussed in numerous papers, see e.g. Refs.17 and 31 and references therein. Recent fits to the TOTEM data with its low ρ value cannot prove or disprove the existence of the odderon until larger values of t, namely those at the dip will be shown to work.

There is little doubt about the existence of the odderon, just because nothing forbids its existence. Its parameters are not predicted from theory. By a plausible estimate, based on the string model, the odderon's slope is roughly $\alpha_0' \approx 2\alpha_P'/3$. The odderon could be detected directly by measuring pp and $\bar{p}p$ differential cross sections at the same energy, e.g. by rescaling the LHC down to the closed Tevatron energy,v $\sim$2 TeV^2.

The pomeron is the central object in forward physics at the LHC. As repeatedly stressed in this paper, in the LHC energy region one for the first time has a chance to identify the pomeron, uncontaminated by secondary exchanges. Perturbative quantum chromodynamics

(pQCD) predicted that the intercept of the (bare) pomeron is much higher than its "canonical" value 0.08.

Finally we note that we ignore the so-called rapidity gap survival corrections that brought much confusion in studies of diffraction dissociation. In our opinion, the confusion comes from the mixture of the space-time treatment of inelastic processes with the analytic S matrix theory, part of which are Regge-poles, operational only for asymptotic states. A reasonable Regge-pole model compatible with unitarity should not contain "rapidity gap survival corrections", otherwise it should be improved within its own formalism. In other words, the size of these corrections reflect the "goodness" of the model.

Acnowledgement

We thank Chung-I Tan and István Szanyi for usfull discussions. L.J. thanks the Organizers of the Montenegro conference on New Trends in High-Energy Physics for their invitation and support.

References

1. S. Donnachie and P.V. Landshoff, Phys. Lett. **B727** (2013) 500, and earlier references therein.
2. D.A. Fagundes, M.J. Menon, and P.V.R.G. Silva, Nucl. Phys. **A966** (2017) 185.
3. D.A. Fagundes, G. Pancheri, A.Grau, S. Pacetti, Y.N. Srivastava, Phys. Rev. **D88** (2013) 094019.
4. V. A. Khoze, A.D. Martin, and M. G. Ryskin, Eur. Phys. J. **C74** (2014) 2756; V. A. Khoze, A. D. Martin, and M. G. Ryskin, Int. J. Mod. Phys. **A30** (2015) 1542004; V.A. Khoze, A.D. Martin, and M.G. Ryskin, Phys. Rev. **D97** (2018) 3,034019.
5. A. Alkin, O. Kovalenko, and E. Martynov, EPL **102** (2013) 3, 31001.
6. A.A. Godizov, Phys. Rev. **D96** (2017) 3, 034023.
7. A.K. Kohara, E. Ferreira, T. Kodama, and M. Rangler, *Description of pp forward elastic scattering at 7 and 8 TeV*, Proc. of EDS Blois 2017: 17th conference on Elastic and Diffractive scattering, Prague, Czech Republic, JUNE 26-30, 2017; A.K. Kohara, E. Ferreira, T. Kodama and M. Rangler, Eur. Phys. J. **C77** (2017) 12, 877.
8. V.S. Fadin, E.A. Kuraev, and L.N. Lipatov, Phys. Lett. **B60** (1975) 50; I.I. Balitsky, L.N. Lipatov, Sov. J. Nucl. Phys. **28** (1978) 822, Yad. Fiz., **28** (1978) 1597.
9. G. Antchev et al. (TOTEM Collab.), Nucl. Phys. **B899** (2015) 527.
10. E.S. Martynov and E. B. Nicolescu, Phys. Lett. **B778** (2018) 414.
11. A. Alkin, O. Kovalenko, and E. Martynov, EPL **102** (2013) 3, 31001.
12. G. Antchev et al. (TOTEM Collab.), (2017), *First determination of the ρ parameter at √s = 13 TeV - probing the existence of a colourless three-gluon bound state*, arXiv:1812.04732; CERN-EP-2017-335; CERN-EP-2017-v3:
13. P. D. B. Collins, *An introduction to Regge Theory and High Energy Physics*, Cambridge University Press (1977).
14. V. Barone and E. Predazzi, *High-energy particle diffraction*, Springer-Verlag Berlin Heidelberg NewYork, ISBN 3540421076, (2002).
15. S. Donnachie, H.G. Dosch, O. Nachtmann, and P. Landshoff, *Pomeron physics and QCD*, Camb. Monogr. Part. Phys. Nucl. Phys. Cosmol. **19** (2002) 1.
16. A.O. Barut and D.E. Zwanziger, Phys. Rev. **127** (1962) 974.
17. L.L. Jenkovszky, Riv. Nuovo Cim. **10N 12** (1987) 1.
18. R. Fiore, L.L. Jenkovszky, V. Magas, F. Paccanoni, and A. Papa, Eur. Phys. J. **A10** (2001) 217.
19. V.N. Gribov and I.Ya. Pomeranchuk, Phys. Rev. Lett. **9** (1962) 238.

20. R. Dolen, D. Horn, and C. Schmid, Phys. Rev. **166** (1968) 1768.
21. G. Veneziano, Nuovo Cim. **A57** (1968) 190.
22. A.I. Bugrij et al. Fortsch. Phys. **21** (1973) 427.
23. R. Fiore, Laszlo L.L Jenkovszky, V. Magas, F. Paccanoni, and A. Papa, Phys. Element. Part. Atom. Nucl. **31** (2000) n° 7B, 47.
24. E.D. Bloom and E.J. Gilman, Phys. Rev. Lett. **25** (1970) 1149; Phys. Rev. **D4** (1971) 2901.
25. P. Desgrolard, L.L. Jenkovszky, and B.V. Struminsky, Phys. Atom. Nucl. **63** (2000) 891, Yad. Fiz. **63** (2000) 962; Eur. Phys. J. **C11** (1999) 145.
26. S.W. MacDowell and A. Martin, Phys. Rev. **135** (1964) B960.
27. M. Capua, S. Fazio, R. Fiore, L.L. Jenkovszky, and F. Paccanoni, Phys. Lett. **B645** (2007) 161.
28. S. Fazio, R. Fiore, L.L. Jenkovszky, and A. Lavorini, Phys. Rev. **D85** (2012) 054009.
29. S. Fazio, R. Fiore, L.L. Jenkovszky, and A. Salii, Phys. Rev. **D90**, (2014) 016007.
30. A. Donnachie and P.V. Landshoff, *Elastic Scattering at the LHC*, arXiv:1112.2485 [hep-ph].
31. L.L. Jenkovszky and I. Szanyi, Phys. Part. Nucl. Lett. **14** (2017) 687.